

## Research Article

# Crystallographically Oriented Nanorods and Nanowires of RF-Magnetron-Sputtered Zinc Oxide

A. K. Srivastava,<sup>1</sup> B. R. Chakraborty,<sup>1</sup> and S. Chandra<sup>2</sup>

<sup>1</sup>National Physical Laboratory, New Delhi 110012, India

<sup>2</sup>Indian Institute of Technology, New Delhi 110016, India

Correspondence should be addressed to A. K. Srivastava, aks@nplindia.ernet.in

Received 11 December 2008; Revised 18 February 2009; Accepted 25 March 2009

Recommended by Ali Eftekhari

The formation of nanoscaled one-dimensional structure constituting the thin films of ZnO via a RF magnetron sputtering process is demonstrated. A detailed analysis of these films has been carried out by exploiting the techniques of ellipsometry, scanning and transmission electron microscopy (SEM, TEM), high-resolution TEM, and scanning tunneling microscopy (STM). The importance of substrate materials due to the nanomorphologies as rods and wires on the substrates as amorphous quartz and silicon, respectively, has been elucidated. It has been exhibited that these fascinating nano-objects (rods, wires) are grown directionally along *c*-axis of hexagonal lattice of ZnO. The nucleation and growth mechanisms of these nano-objects have been discussed to interpret the present results.

Copyright © 2009 A. K. Srivastava et al. This is an open access article distributed under the Creative Commons Attribution License, which permits unrestricted use, distribution, and reproduction in any medium, provided the original work is properly cited.

## 1. Introduction

Semiconducting nanorods and nanowires are indispensable components for the realization of nanoelectronics and exhibit highly tunable optical properties that make them attractive for several applications [1–5]. Among these, ZnO (band gap  $\sim 3.34$  eV) is an important nanostructure with one dimensional (1D) morphology, as it could be the next most important material after the carbon nanotubes. However, unlike the carbon nanotube which can be semiconducting as well as highly metallic, ZnO has the advantage of always being a semiconductor for all its applications. ZnO is a wurtzite hexagonal structure (space group:  $C6mc$ ), with the alternating planes of tetrahedrally coordinated  $O^{2-}$  and  $Zn^{2+}$  stacked along the *c*-axis [6–9]. Due to the unique combination of being piezoelectric, pyroelectric, and a wide-band-gap semiconductor, ZnO is one of the most important MEMS materials for integration in microsystems such as electromechanical coupled sensors and transducers [10–14]. Moreover the material has a potential applicability in monitoring and controlling the environmental conditions, such as the presence of ozone or carbon monoxide in the atmosphere [15, 16]. Keeping in view of its gamut

of applications, it is of importance to fabricate ZnO-1D nanostructures with large surfaces compared to the volume of the material. In the present work, we have grown ZnO films constituted of nanorods/particles on silicon (Si) and nanowires on amorphous quartz, using RF magnetron sputtering.

## 2. Experimental

Film deposition was carried out on Si (diameter: 2 inch, thickness:  $280\ \mu\text{m}$ ) and amorphous quartz (diameter: 1 inch, thickness: 0.5 mm) substrates by RF magnetron in “sputter-up configuration” using a stoichiometric target of ZnO (diameter: 3 inch, thickness:  $\sim 5$  mm) having 99.99% purity. The Si substrates in the present studies were of prime grade, same as those used in semiconductor integrated circuit fabrication. These were chemical-mechanical polished (CMP) by the manufacturer. The average surface roughness (Ra) value, measured using AFM, is in the range of 2–3 Å. Before loading the substrates in the vacuum chamber for sputter deposition, these were cleaned using standard cleaning steps which include: ultrasonic rinsing in

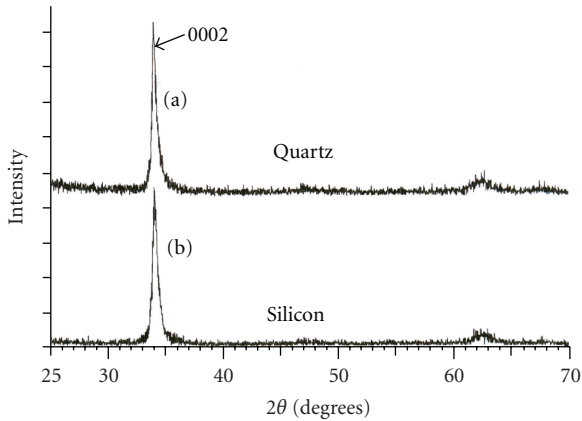


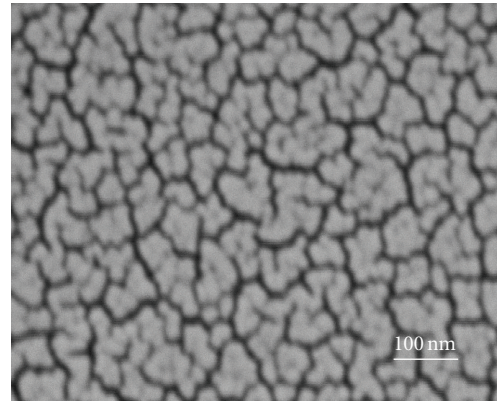
FIGURE 1: XRD patterns of ZnO thin films deposited on (a) amorphous quartz and (b) silicon.

IPA, DI water rinse,  $\text{H}_2\text{SO}_4\text{-H}_2\text{O}_2$ , and dip in dilute HF. The amorphous-quartz substrates were also of the same surface roughness. However in the cleaning procedure for quartz, the dip in dilute HF was omitted to ensure that the surface does not become rough due to etching. The sputtering pressure was maintained at  $1 \times 10^{-2}$  Torr for all the depositions. No external substrate heating was done during deposition. However, substrate temperature rises due to heating in plasma normally up to approximately  $110^\circ\text{C}$ . The details of growth conditions of these films are published elsewhere [17]. During deposition, the sputtering gas: oxygen and argon in 1 : 1 ratio, RF power: 100 W at a frequency of 13.56 MHz, substrate to target distance: 45 mm, and deposition rate:  $140 \text{ \AA}/\text{min}$ , were maintained. Optical absorption data was measured using Shimadzu UV3101 PC spectrophotometer. Ellipsometric parameters were recorded by a Rudolph Research manual null-type ellipsometer (at wavelength: 546.1 nm). X-ray diffractograms were recorded in grazing incidence angle ( $1.5^\circ$ ) geometry by a Bruker AXS D8 Advance diffractometer using  $\text{CuK}\alpha$  wavelength of 1.54059 Å. Microstructural analyses were performed by SEM (model: LEO-440), TEM (models: JEOL TEM 200CX and FEI Tecnai G<sup>2</sup>F30 STWIN) and STM (model: Nano Scope II, Digital Instruments, Inc.).

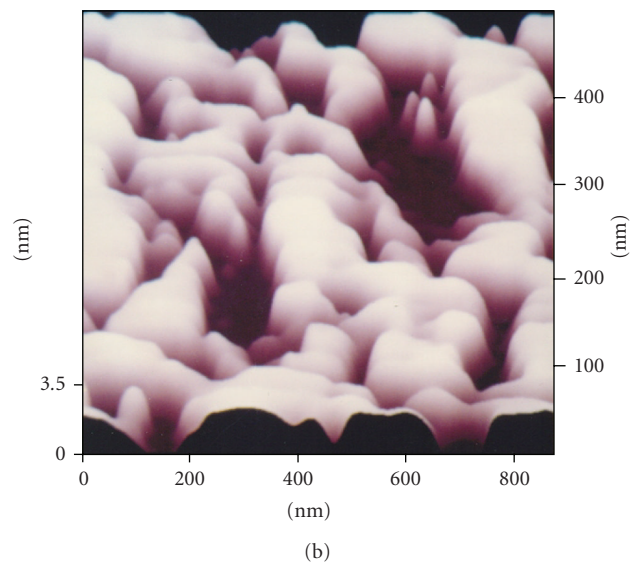
### 3. Results and Discussion

The ellipsometric parameters for the two types of films (Table 1) show that in case of the silicon substrate, the parameters measured at two different surface locations were nearly uniform. The film on quartz substrate has higher value of refractive index and lower thickness for the same duration of deposition. These observations are important for the optical performance of these films.

XRD patterns revealed that the films were crystalline with *c*-axis oriented along 0002 planes (interplanar spacing,  $d = 0.26 \text{ nm}$ ) of hexagonal crystal structure (lattice constants:  $a = 0.32$ ,  $c = 0.52 \text{ nm}$ , JCPDS file # 21-1486) on both substrates (Figure 1). The size of the crystallite as estimated by Scherrer



(a)



(b)

FIGURE 2: Surface topographs of ZnO film deposited on silicon; (a) SEM micrograph and (b) STM image.

formula for films on amorphous quartz and Si substrates was 42 and 31 nm, respectively.

In general SEM topographs have shown a very smooth homogeneous texture of the film with a globular grains consisted of subgrain microstructure. As an illustrative micrograph, (Figure 2(a)) delineates dense grains of size between 10 and 30 nm constituted the entire film on Si substrate. STM measurements with suitable *z*-contrast of Figure 2(b) delineated the contours of energy pits of quantum well type with an average separation of  $\sim 400 \text{ nm}$  between each pit.

TEM studies carried out on the ZnO grown on quartz-substrate exhibited that the film is constituted of fine grain nanoparticles (10–30 nm) coexisting with nanorods of diameter about 20 nm (Figures 3(a), 3(b), 3(c)). The overall appearance of such microstructure definitely states that these films have large surface area, because of the nano-objects present on it and the nano and sub-nanoscale porosity dispersed throughout the film.

TABLE 1: Ellipsometric data of  $n$ ,  $k$ , and  $d$  for the thin films of ZnO.

Substrate	Refractive index ( $n$ )	Extinction coefficient ( $k$ )	Film thickness ( $d$ )
Silicon	$1.41 \pm 0.01$	$0.005 \pm 0.001$	$585 \pm 0.5$ nm
	$1.41 \pm 0.01$	$0.005 \pm 0.001$	$582 \pm 0.7$ nm
Quartz	$2.405 \pm 0.004$	$0.002 \pm 0.001$	$104 \pm 0.5$ nm

Selected area electron diffraction patterns (SADPs) exhibited that although the nanoparticles are randomly arranged with polycrystalline nature, the nanorods are single crystalline. A set of single crystalline SADPs recorded from the nanorods are displayed as Figures 3(d), 3(e). SADP recorded along  $[0001]$  zone axis (Figure 3(d)) shows that the growth of nanorod is along the  $c$ -axis of the hexagonal unit cell. The three important planes  $\bar{1}100$ ,  $01\bar{1}0$ , and  $10\bar{1}0$  are marked as 1, 2, and 3, respectively, on SADP (Figure 3(d)). The growth direction ( $c$ -axis of hexagonal unit cell) is observed frequently on nanorods. An adequate tilting of a nanorod also resulted in a single crystal SADP along  $[2\bar{1}\bar{1}0]$  zone axis (Figure 3(e)). The three important planes  $0001$ ,  $01\bar{1}1$ , and  $01\bar{1}0$  are marked as 4, 5, and 6, respectively, on SADP (Figure 3(e)).

In contrast to quartz substrate, the microstructural features evolved on Si lead to interconnecting faceted nanoparticles of size about 20–40 nm (Figures 4(a), 4(c)). The individual edges/facets of the particles have length of  $\sim 10$ –20 nm with the common boundaries of length  $\sim 20$ –30 nm. The boundaries between the particles are also clean. The nanoparticles are normally aligned in length, resulting as short interconnecting coir-type morphology. Such type of nanoparticles with faceted morphology may be understood on the basis of kinetics of the process during growth, due to a limited period of sputtering. A detailed study in this direction is underway. It is possible that these nanoparticles are originally aligned in the film, and their alignment is disturbed while taking out from the substrate for preparing electron beam transparent thin specimen for examination under the TEM. The nanowired morphology of these microstructures has been observed in the cross-sectional mode, examined under SEM (Figure 4(b)). The diameter of these nanowires measured from SEM micrograph is  $\sim 30$  nm, closely similar to the dimensions of individual nanoparticles resolved under TEM (Figure 4(c)). In a high-resolution TEM mode, it was clearly seen that the growth direction of these wires is along  $c$ -axis due to the stacking of  $0002$  planes ( $d = 0.26$  nm) along this direction (Figure 4(d)).

It is worth noting that the two different types of microstructures of ZnO evolved on different substrates (amorphous-quartz and Si) under similar process conditions. The nanoparticles of a narrow size distribution delineated on Si substrate are useful for obtaining a uniform quality of thin film, which would lead to a consistent performance of any device fabricated by using these films. Such uniform particle size distribution with nanoscaled faceted morphologies originates only when there are a large number of nuclei processing with physically constrained growth. The growth is constrained, and the particles are faceted, which reflects that the preferred planes are developed on

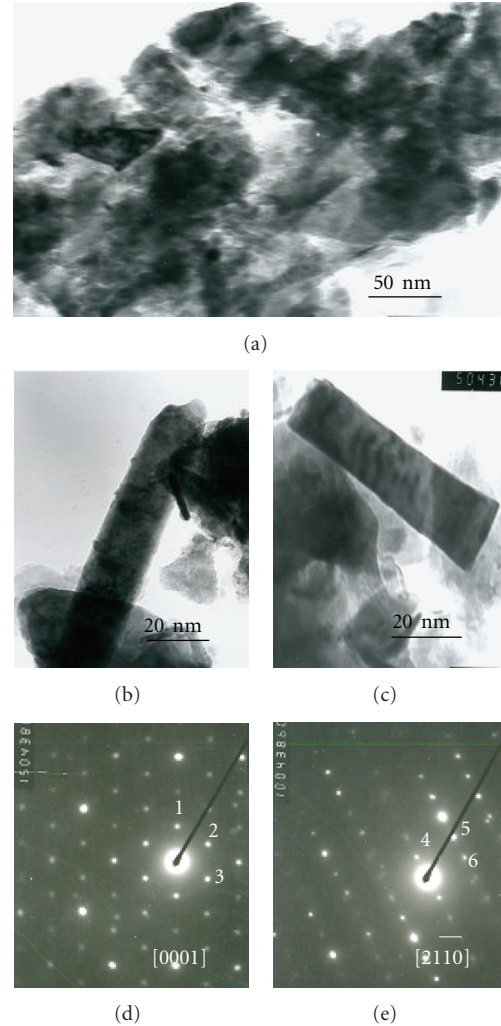


FIGURE 3: TEM micrographs of ZnO film deposited on amorphous-quartz; (a) nanoparticles with flaky microstructure, ((b), (c)) nanorods and ((d), (e)) SADPs along  $[0001]$  &  $[2\bar{1}\bar{1}0]$  zone axes of hexagonal crystal structure.

individual particles, with limited growth. The fascinating morphology of nanoparticles evolved on Si substrate may be understood in the following way. Since the Si is cubic, and the ZnO is hexagonal, the lattice constants of the two materials are therefore very different; the epitaxial growth of nanoparticle on Si is not possible. Under such conditions, large numbers of heterogeneous nuclei can evolve with no directionality governed by the lattice-incoherent substrate; the growth is limited and constrained. However, since the nanoparticles are faceted, it is possible to minimize the

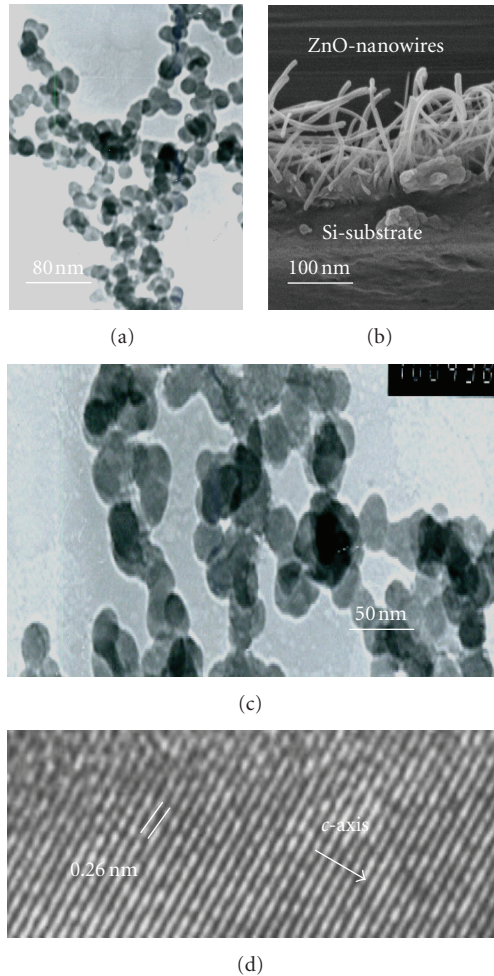


FIGURE 4: TEM micrographs of ZnO film deposited on silicon; ((a), (c)) nanoparticles aligned in wired-morphology, (b) cross-sectional SEM image showing growth of nanowires and (d) a high-resolution TEM image revealing the growth direction of a wire to be  $c$ -axis of hexagonal crystal.

surface energies of the individual facets and to make the system thermodynamically stable; the planes with different surface energies may align to form an aggregate of nanowired morphologies, as observed in the present investigation.

On the contrary, the quartz substrate with amorphous structure at lattice scale lacks any type of ordering at atomic configuration, and therefore a complete mismatch with the freshly deposited hexagonal ZnO is obvious. This phenomenon leads to exceptionally high fraction of ZnO nuclei with no directionality. Such random growth of large number of nuclei leads to very fine particles embedded in fine grained thin film of ZnO. It is surprising to note that these nanoparticles are coexisting with nanorods. Although, there is no understanding about the evolution of these nanorods along with nanoparticles, however, these nanorods are possible only when some of these nano-ZnO nuclei are well oriented in the beginning itself. These oriented nuclei grow in thin films, preferably along  $c$ -axis of the hexagonal unit cell leading to single crystalline rod-like morphology.

Surface changes evolved on these rods may be associated with accumulation of microscale disturbances in the lattice during growth. Since the two kinds of substrates (Si and amorphous quartz) resulted in different types of nanostructured ZnO, the desired electro-optical and sensing properties of these films may also be tailored accordingly.

## 4. Conclusions

RF sputtered growth of ZnO films reveal two important pieces of information, namely, (i) growth of the nanograins along preferred directions to form nanorods on amorphous quartz, and (ii) faceting on individual grains at nanoscale leading a nanowired morphology on Si substrate. A definite correlation between these two nanoscopic features at lattice scale is the preferred growth direction of  $c$ -axis of hexagonal ZnO in both cases. It is possible that the growth in preferred direction may be accompanied with texturing to establish the nanodimensional stability in the microstructure during growth of the film.

## Acknowledgments

The authors are thankful to Dr. Rasmi and Mr. K. N. Sood for XRD and SEM measurements, respectively. Prof. S. Toyoda of Okayama University of Science, Okayama (Japan) is acknowledged for many useful discussions. The Indo-Japanese collaborative project (Ref. DST/INT/JAP/MISC/08) is gratefully acknowledged.

## References

- [1] H. Gleiter, "Nanostructured materials: basic concepts and microstructure," *Acta Materialia*, vol. 48, no. 1, pp. 1–29, 2000.
- [2] H. S. Nalwa, *Handbook of Nanostructured Materials and Nanotechnology*, Academic Press, Tokyo, Japan, 2000.
- [3] F. Carlier, S. Benrezzak, Ph. Cahuzac, et al., "Dynamics of polymorphic nanostructures: from growth to collapse," *Nano Letters*, vol. 6, no. 9, pp. 1875–1879, 2006.
- [4] Z. W. Pan, Z. R. Dai, and Z. L. Wang, "Nanobelts of semiconducting oxides," *Science*, vol. 291, no. 5510, pp. 1947–1949, 2001.
- [5] X. Y. Kong, Y. Ding, R. Yang, and Z. L. Wang, "Single-crystal nanorings formed by epitaxial self-coiling of polar nanobelts," *Science*, vol. 303, no. 5662, pp. 1348–1351, 2004.
- [6] H. Bahadur, A. K. Srivastava, R. K. Sharma, and S. Chandra, "Morphologies of sol-gel derived thin films of ZnO using different precursor materials and their nanostructures," *Nanoscale Research Letters*, vol. 2, no. 10, pp. 469–475, 2007.
- [7] Ü. Özgür, Ya. I. Alivov, C. Liu, et al., "A comprehensive review of ZnO materials and devices," *Journal of Applied Physics*, vol. 98, no. 4, Article ID 041301, pp. 1–103, 2005.
- [8] A. K. Srivastava, K. N. Sood, K. Lal, and R. Kishore, "A process for manufacturing nano-structured zinc oxide tetrapods," Patent filed ref. no. 0773DEL2005, March 2005.
- [9] A. K. Srivastava, N. Gupta, K. Lal, K. N. Sood, and R. Kishore, "Effect of variable pressure on growth and photoluminescence of ZnO nanostructures," *Journal of Nanoscience and Nanotechnology*, vol. 7, no. 6, pp. 1941–1946, 2007.

- [10] A. K. Srivastava, S. A. Agnihotry, and M. Deepa, "Sol-gel derived tungsten oxide films with pseudocubic triclinic nanorods and nanoparticles," *Thin Solid Films*, vol. 515, no. 4, pp. 1419–1423, 2006.
- [11] A. K. Srivastava, "Direct evidence for electron beam irradiation-induced phenomena in nanowired ZnO thin films," *Materials Letters*, vol. 62, no. 27, pp. 4296–4298, 2008.
- [12] A. Hashimoto, K. Suenaga, A. Gloter, K. Urita, and S. Iijima, "Direct evidence for atomic defects in graphene layers," *Nature*, vol. 430, no. 7002, pp. 870–873, 2004.
- [13] K. Urita, K. Suenaga, T. Sugai, H. Shinohara, and S. Iijima, "In situ observation of thermal relaxation of interstitial-vacancy pair defects in a graphite gap," *Physical Review Letters*, vol. 94, no. 15, Article ID 155502, 4 pages, 2005.
- [14] H. Bahadur, A. K. Srivastava, A. K. Rashmi, and S. Chandra, "Effect of sol strength on growth, faceting and orientation of sol-gel derived ZnO nanostructures," *IEEE Sensors Journal*, vol. 8, no. 6, pp. 831–836, 2008.
- [15] R. Martins, E. Fortunato, P. Nunes, et al., "Zinc oxide as an ozone sensor," *Journal of Applied Physics*, vol. 96, no. 3, pp. 1398–1408, 2004.
- [16] M. Kudo, T. Kosaka, Y. Takahashi, H. Kokusen, N. Sotani, and S. Hasegawa, "Sensing functions to NO and O<sub>2</sub> of Nb<sub>2</sub>O<sub>5</sub>- or Ta<sub>2</sub>O<sub>5</sub>-loaded TiO<sub>2</sub> and ZnO," *Sensors and Actuators B*, vol. 69, no. 1, pp. 10–15, 2000.
- [17] R. Singh, M. Kumar, and S. Chandra, "Growth and characterization of high resistivity c-axis oriented ZnO films on different substrates by RF magnetron sputtering for MEMS applications," *Journal of Materials Science*, vol. 42, no. 12, pp. 4675–4683, 2007.